# Hydrogen bonds and van der Waals forces in ice at ambient and high pressures

Biswajit Santra[1], Jiří Klimeš[2,3,4], Dario Alfè[2,4,5,6], Alexandre Tkatchenko[1],
Ben Slater[3,4], Angelos Michaelides[2,3,4],*, Roberto Car[7], and Matthias Scheffler[1]

[1]*Fritz-Haber-Institut der Max-Planck-Gesellschaft, Faradayweg 4-6, 14195 Berlin, Germany*
[2]*London Centre for Nanotechnology, University College London, London WC1E 6BT, UK*
[3]*Department of Chemistry, University College London, London WC1E 6BT, UK*
[4]*Thomas Young Centre, University College London, London WC1E 6BT, UK*
[5]*Department of Physics and Astronomy, University College London, London WC1E 6BT, UK*
[6]*Department of Earth Sciences, University College London, London WC1E 6BT, UK*
[7]*Department of Chemistry, Princeton University, Princeton, New Jersey 08544, USA*

The first principles approaches, density functional theory (DFT) and quantum Monte Carlo, have been used to examine the balance between van der Waals (vdW) forces and hydrogen (H) bonding in ambient and high pressure phases of ice. At higher pressure, the contribution to the lattice energy from vdW increases and that from H bonding decreases, leading vdW to have a substantial effect on the transition pressures between the crystalline ice phases. An important consequence, likely to be of relevance to molecular crystals in general, is that transition pressures obtained from DFT functionals which neglect vdW forces are greatly overestimated.

Water-ice, the most common molecular solid in nature, exhibits a rich and complex phase diagram. At present this includes ice Ih, ice Ic and 14 other crystalline ice phases [1, 2]. Although the phase diagram of ice up to around 2 GPa is well-established experimentally, understanding of the subtle balance of intermolecular interactions which give rise to this richness is incomplete. In particular, the relative contribution of hydrogen (H) bonding and van der Waals (vdW) dispersion forces to the cohesive properties of the various crystalline ice phases is still not understood. From a theoretical perspective, the varied densities of experimentally characterized ice crystal structures, with the molecules fixed on well-defined lattices, affords an excellent opportunity to quantify and assess the nature of these intermolecular interactions.

Computer simulation techniques have proved instrumental in understanding ice (e.g. [3–14]). In particular, density-functional theory (DFT) with generalized gradient approximation (GGA) functionals has been widely applied. Certain GGAs describe the ambient pressure ice Ih phase reasonably well [9] and predict the proton order–disorder phase transition temperatures between ice Ih and XI and ice VII and VIII in good agreement with experiments [6]. However, it is known that GGAs suffer deficiencies when vdW forces are important and indeed it has been suggested that this is the reason certain GGAs produce a liquid water density about 15–20% less than experiment [15–17] or fail to predict the correct ground state structure for some small water clusters [18]. Despite the considerable body of DFT work on ice phases, the role of vdW forces and H bonding has not been systematically examined in anything other than ice Ih [19, 20]. However, with recent developments (e.g. [21–23]), it is now possible to tackle this issue head on and estimate the importance of vdW forces and H bonding in the various phases of ice.

TABLE I. Absolute lattice energies (omitting zero point energy effects) of ice Ih, II, and VIII. Relative energies compared to ice Ih ($\Delta U_0$) are given in parenthesis. All values are in meV/$H_2O$.

|  | Ih | II | VIII |
|---|---|---|---|
| Expt.[a] | -610 | -609 (1) | -577 (33) |
| DMC | -605 $\pm 5$ | -609 $\pm 5$ (-4) | -575 $\pm 5$ (30) |
| PBE | -636 | -567 (69) | -459 (177) |
| PBE0 | -598 | -543 (55) | -450 (148) |
| PBE0+vdW$^{TS}$ | -672 | -666 (6) | -596 (76) |

[a] Ref. [24], with zero point energy contributions removed.

Here we report an extensive series of first principles studies aimed at better understanding the role of vdW and H bonding in ice. This includes DFT calculations with and without a treatment of vdW forces on the ambient pressure phase of ice, ice Ih, and all the proton ordered phases, namely, in order of increasing pressure, ice IX, II, XIII, XIV, XV, VIII. We also report diffusion quantum Monte Carlo (DMC) calculations for ice Ih, II, and VIII as reference values to complement the experimental results. DMC is highly accurate for weak interactions including vdW bonded systems and represents the state-of-the-art for electronic structure simulations of solids. From this work we find that the contribution of vdW to the cohesive properties of ice increases as one moves to the higher density phases, whereas the contribution from H bonds decreases. As a result, vdW plays a crucial role in determining the relative stabilities and phase transition pressures in ice. The results presented here are likely to be of relevance to understanding intermolecular interactions in water in all its condensed phases as well as to structural searches for (novel) high pressure ices and to molecular crystals in general.

We start by discussing lattice energies, which are obtained by subtracting the total energy [25] of the ice unit
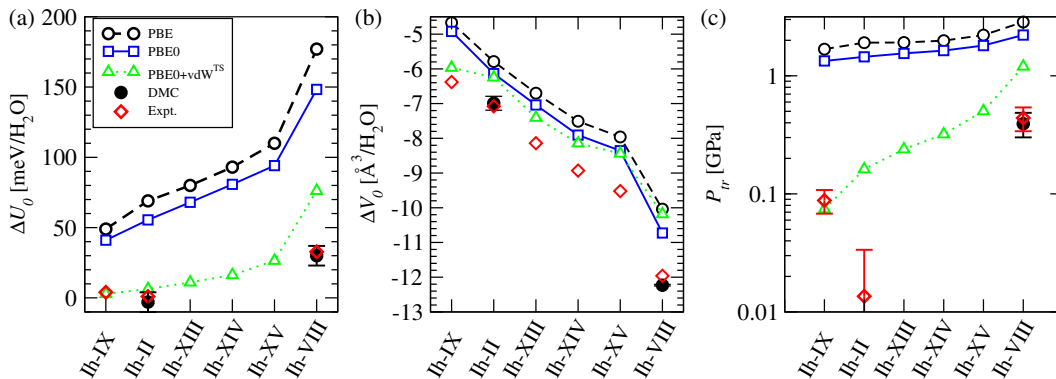
* angelos.michaelides@ucl.ac.uk

FIG. 1. Relative lattice energies, $\Delta U_0$ (a), and volumes, $\Delta V_0$ (b), of the high pressure ice phases with respect to the lattice energy of ice Ih obtained with the methods indicated. (c) Transition pressures ($P_{tr}$) from ice Ih to the various high pressure phases.

cell containing $n$ $H_2O$ molecules from the total energy of $n$ isolated $H_2O$ molecules. In this context Whalley's extrapolations of the experimental finite temperature and pressure phase coexistence lines to zero temperature and pressure are extremely valuable [24]. For the proton ordered phases Whalley considered, these indicate that ice IX, II, and VIII are less stable than ice Ih by only $3.5 \pm 0.8$, $0.6 \pm 1.0$, and $33$ meV/$H_2O$, respectively [24]. These values agree well with DMC. Specifically, DMC predicts that ice VIII is $30 \pm 7$ meV/$H_2O$ less stable than ice Ih. Similarly, the near energetic degeneracy between ice Ih and ice II is captured with DMC, and within the DMC error bars, ice Ih and ice II are equally stable. From Table I it can also be seen that DMC lattice energies are in very good agreement with experiment as well. Overall this gives us confidence in the quality of Whalley's experimental extrapolations and the accuracy of the DMC calculations. This therefore provides an excellent basis for exploring the role of H bonds and vdW in ice with DFT.

We now discuss the results obtained with PBE [26], one of the most widely used functionals. For ice Ih, PBE yields a reasonable lattice energy of about $640$ meV/$H_2O$, an overestimate of around $30$ meV/$H_2O$ which is consistent with previous work [9]. However, Table I and Fig. 1(a) reveals a severe deterioration in the performance of PBE for the higher density phases. Whereas experiment and DMC suggest that the energy difference between ice Ih and the least stable ice VIII phase is about $30$ meV/$H_2O$, PBE gives $\sim 180$ meV/$H_2O$ difference. This is mainly because PBE underestimates the stability of the high pressure phases, suggesting that attractive interactions, more important in the higher density ice phases, are not captured accurately with PBE. In addition to substantially overestimating the energy differences between the various phases, the changes in volumes ($\Delta V_0$) upon going from ice Ih to the high pressure phases are also underestimated with PBE (Fig. 1(b)) and critically the transition pressures ($P_{tr}$) — obtained from $P_{tr} = -\Delta U_0 / \Delta V_0$ — are $\sim 5$-$15$ times larger than

experiment (Fig. 1(c)).

Seeking to understand why PBE performs so poorly for the high pressure ice phases, we have considered various potential sources of errors. First we analyzed the dipole moment and polarizability of an isolated water molecule. PBE, like other GGAs, overestimates the polarizability of an isolated water molecule by $\sim 10\%$ compared to experiment, which is related to any overly delocalized electron density and a too small HOMO-LUMO gap. Incorporation of a fraction of Hartree-Fock exchange in to the GGAs is an established approach for alleviating this problem. In particular, a popular PBE-based hybrid functional, PBE0 [27], widens the HOMO-LUMO gap of the isolated water molecule by $\sim 40\%$ and provides more accurate polarizabilities and interaction energies within a variety of water clusters [28–30]. When applied to ice, the lattice energies obtained with PBE0 (Table I) are indeed improved over PBE, however, the energy difference between ice Ih and ice VIII is still about four times larger than the experimental value. In addition, as with PBE, upon going from ice Ih to the high pressure phases the transition pressures are about an order of magnitude too large compared to experiment (Fig. 1(c)).

Turning to the role of H bonding, the relative H bond strength has been estimated from shifts in the O-H stretching frequencies, which is a simple and widely used measure of H bond strength (e.g. [31]). Specifically, the softening (red-shift) of the intramolecular O-H stretching frequencies in the various phases is compared to the (average) O-H stretching frequency of an isolated water monomer [32]. Based on the available experimental frequencies for several of the phases [33–35], H bonds get weaker with increasing pressure. This established, but not necessarily obvious, result arises because the nearest neighbor water-water distances get larger as one moves from ice Ih with its open ring structure to the more complex higher pressure phases. In line with previous calculations [36], PBE reproduces the trend in frequency changes with pressure but the red-shift (i.e., strength) compared to the the isolated water molecule is signifi-

cantly overestimated compared to experiment, particularly for ice Ih (see Fig. 2(a)). PBE0 predicts frequency shifts in much better agreement with experiment (Fig. 2(a)). However, as we have seen, the relative stabilities of the ice phases with PBE0 are significantly in error, which clearly suggests that H bonds are not the only important interaction in the high density phases.

We now consider the influence of vdW interactions with the scheme of Tkatchenko and Scheffler (referred to as vdW$^{TS}$), in which an additional $C_6/R^6$ tail is added to the DFT total energy, with the $C_6$ coefficients calculated as functionals of the electron density [22]. Dramatic improvements in the relative energies of the various phases and phase transition pressures are observed (Fig. 1). In particular, upon going from PBE0 to PBE0+vdW$^{TS}$ the energy difference between ice Ih and ice II is reduced to just 6 meV/H$_2$O and, likewise, ice VIII is now only 76 meV/H$_2$O less stable than ice Ih. As a consequence, with vdW the ice Ih to ice II transition pressure is reduced by more than one order of magnitude and is in good agreement with experiment. Similarly, the ice Ih to ice VIII transition comes within a factor of two of experiment. The substantially improved transition properties when vdW is accounted for results from a strong dependence of vdW on density, as shown in Fig. 2(b). Clearly as the density of the ice phases increases, so too does the vdW contribution to the lattice energy and indeed for the highest density phase (ice VIII) the vdW contribution is about twice what it is in ice Ih. Overall the decrease of H bond strength and the increase of vdW in the high pressure phases clearly shows a significant enhancement of relative contribution of vdW over H bonding interactions for the cohesive properties of the high pressure ice phases.

Our findings regarding the importance of vdW for the high-pressure phases of ice also hold when using functionals based on the vdW-DF approach of Dion *et al.* [21, 37]. The phase transition pressures obtained with such functionals are similar to those obtained with the TS scheme. Both approaches neglect the non-additive many-body vdW energy beyond the pairwise approximation. We have found that the many-body vdW energy plays a minor role for the different phases of ice by using an extension of the TS scheme [38]. Also we find that quantum effects based on zero point energies play a minor role in determining the relative stabilities of the various phases. Specifically, the zero point energies of the different phases (calculated with PBE and the harmonic approximation) differ by <10 meV/H$_2$O.

We now discuss why vdW interactions play a crucial role in determining the relative stabilities of the various ice phases. For any two non-bonded atoms vdW forces result from an induced dipole-induced dipole interaction whose leading term varies as $C_6R^{-6}$. At a given $R$, vdW will increase if the polarizability of the atoms increases, i.e., $C_6$ becomes larger and/or the number density of the atoms increases. Our calculations with the TS approach show that the $C_6$ coefficients do indeed increase upon go-
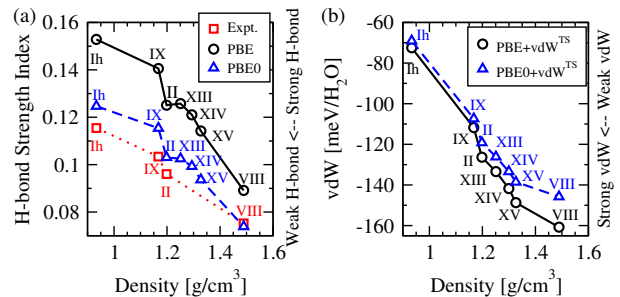


FIG. 2. (a) H bond strength index [32] and (b) vdW energy contributions plotted as a function of the experimental densities of the ice phases at zero pressure. Experimental values are taken from [33–35].

ing from ice Ih to ice VIII, by 24% for H and 6% for O. However, the major effect that leads to an increase in the vdW interactions in the high density phases is simply the higher packing of water molecules. This can be seen by comparing the O-O radial distribution functions of ice Ih with e.g. ice II and ice VIII (Fig. 3(a)). Although ice Ih possesses the shortest nearest neighbor O-O distances, the structure is open and there is a large gap of $\sim$2 Å between the first and second coordination shells. In contrast, in the high density phases the second and subsequent coordination shells appear at much shorter O-O separations. In fact in ice VIII, which is comprised of two interpenetrating sub-lattices, the first and second coordination shells fall almost on top of each other (with the shortest O-O distances associated with non H bonded contacts). The higher packing, particularly in the *ca.* 3 to 6 Å regime is reflected by the integrated number of neighbors versus O-O distance shown in Fig. 3(b)). Overall these additional molecules at short (ice VIII) and intermediate (ice II) distances lead to enhanced vdW interactions in the high pressure phases. Fig. 3(c) provides a more quantitative basis for the above argument, by showing the total vdW interactions — as obtained from the TS scheme — for ice Ih, II and VIII in the range of *ca.* 3 Å to 6 Å. It can be seen that beyond about *ca.* 3 Å there are more substantial contributions from vdW from ice II and VIII than ice Ih. Although vdW is generally considered to be a long range interaction, the dominance of vdW in this *ca.* 3 Å to 6 Å regime is to be expected given that the sum of the vdW radii of O and H in the condensed phase (calculated with TS scheme) is only $\leq$3 Å. Note that in fact the difference in the vdW contribution between the various phases is essentially converged to the periodic limit after about 8 Å.

In conclusion, we have performed an extensive first principles study of ice at ambient and high pressures. From the ambient to the high pressure phases the contribution to the lattice energy arising from vdW forces monotonously increases. This has a significant impact on the phase transition pressures, as exemplified by calculations with conventional $xc$ functionals where vdW forces are not accounted for, and where transition pres-
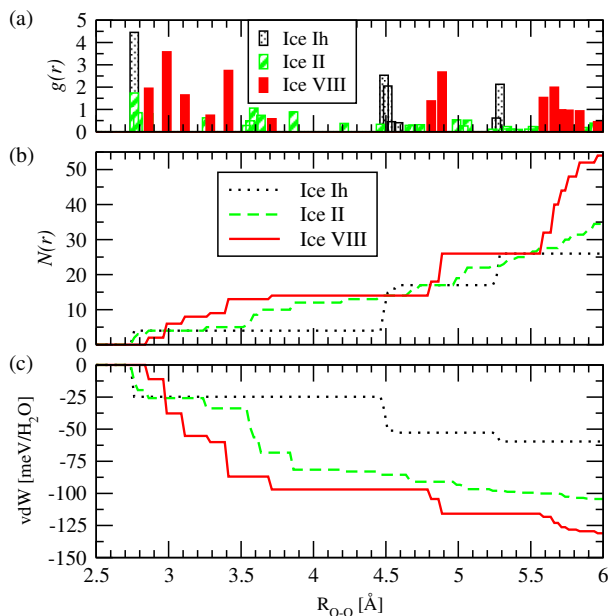
FIG. 3. (a) O-O radial distribution functions ($g(r)$) of ice Ih, ice II, and ice VIII. (b) Integrated number of neighbors ($N(r)$) and (c) vdW contributions (obtained from the TS scheme) as a function of O-O distance for the same three phases.

worthwhile to stress that there certainly remains scope for further improvements within DFT in terms of transition pressures, absolute lattice energies and volumes for ice. In particular, there is scope for improving the lattice energy of ice VIII obtained with vdW$^{TS}$, with the current underestimation in the lattice energy possibly associated with the radically different structure of ice VIII compared to the other phases considered. The strong dependence of vdW interactions on density suggests that even at ambient pressure, vdW forces will also be important to liquid water which has a $\sim$8% higher density than ice Ih. Indeed this is consistent with a number of recent DFT studies [16, 17]. Although vdW is often associated with so-called "sparse" matter we have shown that it attains greater significance at high density. This somewhat counterintuitive result arises because vdW forces mainly enhance interactions between molecules at medium range (i.e., second and third coordination shells at 3 to 6 Å separations). Therefore, analogous effects are expected for water in other environments such as in confined geometries, interfaces, and clathrates, and indeed for other hydrogen bonded molecular crystals at high pressure.

sures more than one order of magnitude larger than experiment are obtained. By accounting for vdW forces, the phase transition pressures more closely agree with experiment. This finding provides a new physical insight and is also relevant to DFT-based structural searches for novel ice polymorphs [14, 39], by implying that a reexamination of the high pressure region of the ice phase diagram with a vdW corrected DFT approach would be worthwhile. Whilst the focus of the current study has been on understanding the role of H bonding and vdW forces in ice, rather than on improving the current state-of-the-art in DFT simulations for water, it is nonetheless

[1] C. G. Salzmann *et al.*, Phys. Rev. Lett. **103**, 105701 (2009); and references therein.
[2] O. Mishima *et al.*, Nature **314**, 76 (1985).
[3] C. Lee *et al.*, Phys. Rev. Lett. **69**, 462 (1992).
[4] D. R. Hamann, Phys. Rev. B **55**, R10157 (1997).
[5] E. Sanz *et al.*, Phys. Rev. Lett. **92**, 255701 (2004).
[6] S. J. Singer *et al.*, Phys. Rev. Lett. **94**, 135701 (2005).
[7] G. A. Tribello, B. Slater, and C. G. Salzmann, J. Am. Chem. Soc. **128**, 12594 (2006).
[8] M. de Koning *et al.*, Phys. Rev. Lett. **96**, 075501 (2006).
[9] P. J. Feibelman, Phys. Chem. Chem. Phys. **10**, 4688 (2008).
[10] A. Hermann and P. Schwerdtfeger, Phys. Rev. Lett. **101**, 183005 (2008).
[11] D. Pan *et al.*, Phys. Rev. Lett. **101**, 155703 (2008).
[12] A. Erba *et al.*, J. Phys. Chem. B **113**, 2347 (2009).
[13] J. A. Morrone *et al.*, J. Chem. Phys. **130**, 204511 (2009).
[14] B. Militzer and H. F. Wilson, Phys. Rev. Lett. **105**, 195701 (2010).
[15] I.-C. Lin *et al.*, J. Phys. Chem. B **113**, 1127 (2009).
[16] J. Schmidt *et al.*, J. Phys. Chem. B **113**, 11959 (2009).
[17] J. Wang *et al.*, J. Chem. Phys. **134**, 024516 (2011).
[18] B. Santra *et al.*, J. Chem. Phys. **129**, 194111 (2008).
[19] I. Hamada, J. Chem. Phys. **133**, 214503 (2010).
[20] F. Labat, C. Pouchan, C. Adamo, and G. E. Scuseria, J. Comput. Chem. **32**, 2177 (2011).
[21] M. Dion *et al.*, Phys. Rev. Lett. **92**, 246401 (2004).
[22] A. Tkatchenko and M. Scheffler, Phys. Rev. Lett. **102**, 073005 (2009).
[23] S. Grimme *et al.*, J. Chem. Phys. **132**, 154104 (2010).
[24] E. Whalley, J. Chem. Phys. **81**, 4087 (1984).
[25] The FHI-aims [40] and VASP [41, 42] codes have been used for the DFT calculations. DMC calculations were performed using CASINO [43] within the fixed node pseu-

dopotential approximation and B-spline basis sets [44]. Further details can be found in the supplementary material.

[26] J. P. Perdew, K. Burke, and M. Ernzerhof, Phys. Rev. Lett. **77**, 3865 (1996).

[27] C. Adamo and V. Barone, J. Chem. Phys. **110**, 6158 (1999).

[28] J. R. Hammond *et al.*, J. Chem. Phys. **131**, 214103 (2009).

[29] B. Santra, A. Michaelides, and M. Scheffler, J. Chem. Phys. **127**, 184104 (2007); *ibid* **131**, 124509 (2009).

[30] F.-F. Wang *et al.*, J. Chem. Phys. **132**, 134303 (2010).

[31] X.-Z. Li, B. Walker, and A. Michaelides, Proc. Natl. Acad. Sci. USA **108**, 6369 (2011).

[32] The H bond strength index is calculated as $(\nu_{\mathrm{O-H}}^{\mathrm{H_2O}} - \nu_{\mathrm{O-H}}^{\mathrm{ice}})/\nu_{\mathrm{O-H}}^{\mathrm{H_2O}}$, where $\nu_{\mathrm{O-H}}^{\mathrm{H_2O}}$ and $\nu_{\mathrm{O-H}}^{\mathrm{ice}}$ are the average uncoupled covalent O-H stretching frequencies of an isolated $H_2O$ molecule and ice, respectively. When there is no H bond the index is zero. Frequency shifts are just one measure of relative H bond strength. Other key quantities related to HB strength, e.g., water molecule dipole moments and covalent O-H bond lengths, also decrease from the low to the high density phases.

[33] J. E. Bertie and E. Whalley, J. Chem. Phys. **40**, 1646 (1964).

[34] J. E. Bertie and F. E. Bates, J. Chem. Phys. **67**, 1511 (1977).

[35] P. T. T. Wong and E. Whalley, J. Chem. Phys. **64**, 2359 (1976).

[36] M. V. Vener *et al.*, Chem. Phys. Lett. **500**, 272 (2010).

[37] J. Klimeš, D. R. Bowler, and A. Michaelides, J. Phys.: Cond. Matt. **22**, 022201 (2010).

[38] A. Tkatchenko *et al.*, to be published.

[39] C. J. Pickard and R. J. Needs, J. Chem. Phys. **127**, 244503 (2007).

[40] V. Blum *et al.*, Comp. Phys. Comm. **180**, 2175 (2009).

[41] G. Kresse and J. Hafner, Phys. Rev. B **47**, 558 (1993).

[42] G. Kresse and J. Furthmüller, Phys. Rev. B **54**, 11169 (1996).

[43] R. J. Needs *et al.*, J. Phys.: Condensed Matter **22**, 023201 (2010).

[44] D. Alfè and M. J. Gillan, Phys. Rev. B **70**, 161101 (2004).